Spatial transcriptomics reveals tissue-specific gene expression in supraspinatus muscle after rotator cuff tear and repair in the pre-clinical rabbit model

Severin Ruoss[1], Chanond A. Nasamran[1], Mary C. Esparza[1], Kathleen M. Fisch[1], Adam J. Engler[1], Samuel R. Ward[1]
[1]University of California San Diego, La Jolla, CA
severin.ruoss@gmail.com

Disclosures: The authors have nothing to disclose.

INTRODUCTION: RNA sequencing (RNAseq) has been used recently to define skeletal muscle tissue states, to track disease progression and healing responses, and to investigate mechanisms-of-action of treatments in clinical settings. Unfortunately, changes in tissue and cellular composition seen in conditions affecting skeletal muscle prevent us from understanding individual cell biology with whole-tissue RNA sequencing data. Conversely, single-cell and single-nuclei RNAseq cannot address this problem because muscle cells are multinucleated and too large to be encapsulated in droplet-based methods. Using spatial transcriptomics we make fiber type- and connective tissue-specific comparisons to reveal and localize differentially expressed genes (DEGs) along the time course of healthy, torn, and repaired supraspinatus muscle in the pre-clinical rabbit model of rotator cuff tear.

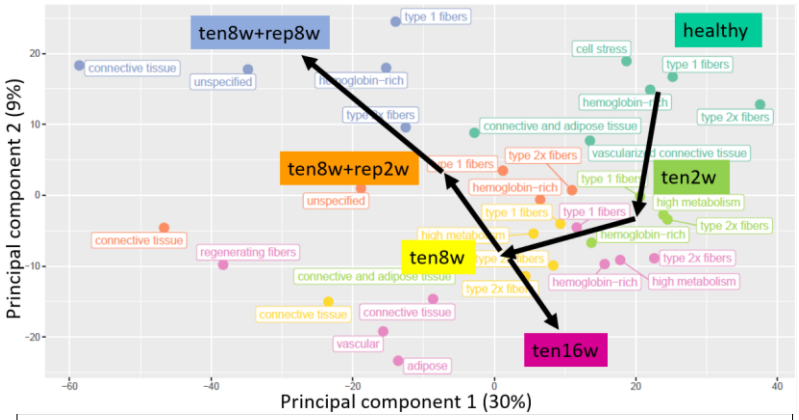

Fig. 1. Principal component analysis of all clusters and samples. N = 20.

METHODS: The following 20 snap frozen samples of supraspinatus muscle were used from the rabbit model of rotator cuff tear: 5 healthy, 3 2-weeks after tenotomy (ten2w), 2 8-weeks after tenotomy (ten8w), 5 ten8w + 2 weeks after repair (ten8w+rep2w), 3 ten8w+rep8w, and lastly, 2 non-repaired time-matched ten16w samples. 10 µm sections were mounted onto the Visium slide (10x Genomics) which was pre-coated with capture primers containing spatial barcodes and a Unique Molecular Identifier (UMI) sequence. After hematoxylin & eosin staining and imaging, libraries were prepared and then sequenced on a Novaseq 6000 (Illumina). Images were manually aligned using Loupe Browser 5.0 (10X Genomics). Spatial feature counts were generated using Space Ranger 1.2.0 count by aligning reads to OryCun2.0 with annotations from Ensembl release 104 (Oryctolagus_cuniculus.OryCun2.0.104.chr.gtf). Visium spots were clustered and annotated based on transcriptomic profiles. Spots were then pseudo-bulked by tissue type and replicate. DEGs were calculated using the limma-voom method with the model ~0+celltype_condition. Adjusted p-values < 0.05 were deemed significant for DEG analysis.

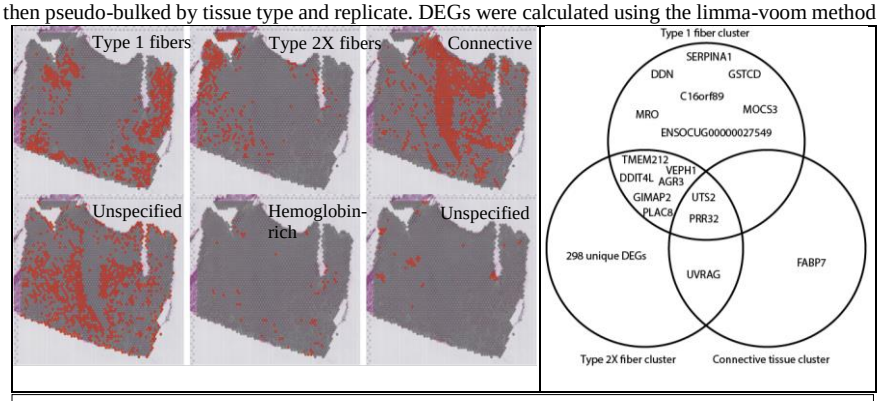

Fig. 2. Unbiased clustering in one sample at ten8w (left) and Venn diagram showing DEGs of type 1, type 2X, and connective tissue clusters at ten8w vs. ten8w+rep2w (right).

RESULTS SECTION: Type 1 fiber-, type 2X fiber-, connective tissue, and hemoglobin-rich clusters were identified at every time point based on high expression of the marker genes MYH7, MYH1, COL1A2, and GLNB2, respectively. Additionally, clusters indicating different metabolic activity (ATP6, ND2, COX3) were identified at ten2w, ten8w, and ten16w, and more vascularized areas (ACTA2, MYH11) were detected at baseline and ten16w, and one cluster indicating cell stress (ANKRD1, HSPB1, HSPB8) was found at baseline. A few clusters remained "unspecified" due to lack of conserved marker genes (Fig 1). A directional change of transcriptional expression was observed at the ten8w timepoint dependent on whether the tear was repaired or left alone until ten16w (Fig. 1). Surgical repair induced cluster-specific transcriptional changes after 2 weeks (Fig. 2). The type 2 fiber cluster presented with 307 DEGs, 298 of which were cluster-specific (Fig. 2+3). The type 1 fiber cluster presented with 15 DEGs (7 of which were unique) and 4 DEGs were detected in the connective tissue cluster, FABP7 being the only cluster-specific DEG at this time point (Fig. 2).

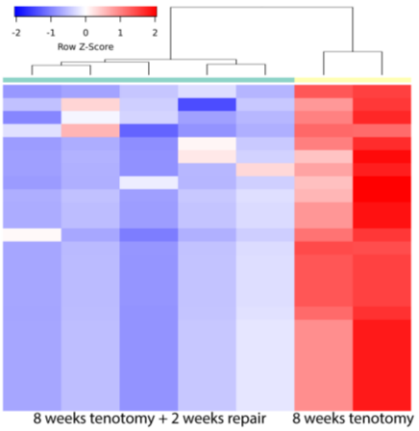

Fig. 3. Top 25 DEGs of type 2X fiber clusters at ten8w vs. ten8w+rep2w. Columns are samples and the dendrogram shows unbiased hierarchical clustering.

DISCUSSION: The presence of cluster-specific DEGs indicates the importance of more detailed mechanistic analyses at the sub-tissue level in heterogenous skeletal muscle (as opposed to whole tissue analysis), especially if relative tissue shares are known to change over the time course of the investigated pathology. Interestingly, most differential transcriptional activity was found in the type 2X fiber-related cluster at 2 weeks after repair (307 DEGs), while only 4 DEGs were detected in the connective tissue cluster, at least at the time point of measurement. Future studies should investigate whether these "asymmetric" transcriptional responses are a function of the time point they were measured in this study, or whether they translate into similarly asymmetric adjustments at the protein or functional levels. One limitation is that adipose accumulation, which is a key feature of chronic rotator cuff tears and detected on H&E staining, often did not yield separate clusters; these areas were then represented within connective tissue-rich clusters after unbiased clustering. This was likely due to the method's limited resolution and relative connective tissue abundance between adipocytes (data not shown).

SIGNIFICANCE/CLINICAL RELEVANCE: Tendon tears, chronic low back pain, dystrophies, sarcopenia, whiplash, and many other conditions affecting skeletal muscle result in intramuscular adipose and connective tissue accumulation. Our data suggests that different tissues within the same organ may respond differently to a treatment (here, surgical tendon repair); thus, measuring effects at the sub-tissue level may lead to better mechanistic understanding and ultimately help develop more informed treatments.